Heat transfer characteristics of a rectangular natural circulation loop containing solid-liquid phase-change material suspensions

Received September 2003
Revised August 2004
Accepted October 2004

C.J. Ho, S.Y. Chiu and J.F. Lin
Department of Mechanical Engineering, National Cheng Kung University, Tainan, Taiwan, Republic of China

Abstract

Purpose – To examine the heat transfer characteristics of soild-liquid phase change material (PCM) suspensions in a rectangular natural circulation loop.

Design/methodology/approach – A continuum mixture flow model is used for the buoyancy-driven circulation flow of the PCM suspensions together with an approximate enthalpy model to describe the solid-liquid phase change (melting/freezing) process of the PC particles in the loop. Numerical simulations *via* a finite difference method have been conducted for the pertinent physical parameters of a loop with fixed geometrical configuration in the following ranges: the modified Rayleigh number $Ra^* = 10^9$-10^{13}, the modified Stefan number $Ste^* = 0.05$-0.5, the particle volumetric fraction $C_v = 0$-20 percent and the modified subcooling factor $Sb^* = 0$-2.0.

Findings – The melting/freezing processes of the PCM particles at the heated/cooled sections of the loop are closely interrelated in their inlet conditions of the suspension. The influences of the modified Rayleigh number, the particle fraction, the modified Stefan number, and the modified subcooling factor on the heat transfer behavior, as well as the thermal efficacy of the PCM suspensions are elucidated. There could be a flow regime in the parametirc domain where heat transfer performance of the suspension circulation loop is significantly enhanced, due to contribution of the latent heat transport associated with melting/freezing of PCM particles.

Research limitations/implications – Future work to address effects of the geometric parameters such as the aspect ratio; the lengths and locations of, as well as the relative height between the heated and cooled sections is definitely needed, which are necessary steps towards developing more reliable predictive tools for system design of a circulation loop containing PCM suspension.

Originality/value – This work has explored the feasibility and quantified the efficacy of incorporating the PC suspensions as the heat transfer enhancement medium in a natural circulation loop, which has not been examined previously.

Keywords Heat transfer, Flow, Numerical analysis, Simulation

Paper type Research paper

The authors gratefully acknowledge the support from National Science Council of ROC in Taiwan through Project Nos. NSC-90-2212-E006-084 and NSC-91-2212-E006-133. The computing facility and time for this work were partially provided by the National Center for High Performance Computing of NSC and is gratefully acknowledged.

International Journal of Numerical Methods for Heat and Fluid Flow
Vol. 15 No. 5, 2005
pp. 441-461

0961-5539
DOI 10.1108/09615530510593639

Nomenclature

AR = aspect ratio of rectangular loop, l_H^+/l_V^+
Bi_p = Biot number of PCM particle, Ur_p^+/k_p
c_p = specific heat
c_v = volumetric fraction of PCM particles
h = heat transfer coefficient
h_{ls} = latent heat of fusion
k = thermal conductivity
k^*_{bf} = thermal conductivity ratio, k_b/k_f
k^*_{pf} = thermal conductivity ratio, k_p/k_f
l_c^+ = length of cooled section
l_h^+ = length of heated section
l_h = dimensionless length of heated section, l_h^+/l_c^+
l_H^+ = width of the rectangular loop
l_H = dimensionless width of the rectangular loop, l_H^+/l_c^+ or $(1 + 2\Delta z)AR/2$
l_L^+ = total length of rectangular loop, $2(l_V^+ + l_H^+)$
l_L = dimensionless total length of rectangular loop, $2(l_v + l_H)$ or $(1 + 2\Delta z)(1 + AR)$
l_V^+ = height of the rectangular loop
l_v = dimensionless height of the rectangular loop, l_V^+/l_c^+ or $(1 + 2\Delta z)/2$
Nu = Nusselt number, $h(2r_i^+)/k_b$
Pr = Prandtl number, ν_b/α_b
q'' = local heat flux
$q''*$ = local dimensionless heat flux, q''/q''_h
R_L = dimensionless pipe radius, r_i^+/l_L^+
Ra* = modified Rayleigh number, $\left(g\beta q''_h r_i^+ l_L^{+3}\right)/(\alpha_b \nu_b k_b)$
Re = Reynolds number, $2r_i^+ u_m^+/\nu_b$ or $2u_m Ra^{*1/4}/Pr$
r^+ = radial coordinate
r_p^+ = radius of PCM particle
r = dimensionless coordinate, r^+/r_i^+
r_p = dimensionless radius of particles, r_p^+/r_i^+
s^+ = axial coordinate
s = dimensionless axial coordinate, s^+/l_c^+
Sb* = modified subcooling factor, $(T_m - T_c)/(q''_h r_i^+/k_b)$
Ste* = modified Stefan number, $C_{p,b}(q''_h r_i^+/k_b)/h_{ls}$
T = temperature
u^+ = velocity in the axial direction
u = dimensionless axial velocity, $u^+/(Ra^{*1/4}\alpha_b/r_i^+)$
Δz^+ = mean relative elevation of the cooling section to the heated section
Δz = dimensionless mean relative elevation of the cooling section to the heated section, $\Delta z^+/l_c^+$

Greek symbols

α = thermal diffusivity
α^*_{bf} = thermal diffusivity ratio, α_b/α_f
ε_h = effectiveness of convection coefficient enhancement, $\bar{h}_{c,b}/\bar{h}_{c,f}$ or $(\overline{Nu}_{c,b}/\overline{Nu}_{c,f})(k^*_{bf})$
$\varepsilon_{T_{max}}$ = effectiveness of wall temperature reduction, $(T_{w,h,max,f} - T_m)/(T_{w,h,max,b} - T_m)$ or $(\theta_{w,h,max,f}/\theta_{w,h,max,b})(k^*_{bf})$
γ_L = correction factor of the loop length, $l_{L,eff}^+/l_L^+$
ν = kinematic viscosity
θ = dimensionless temperature, $(T - T_m)/(q''_h r_i^+/k_b)$
ρ = density
ρ^*_{bf} = density ratio, ρ_b/ρ_f
ρ^*_{pf} = density ratio, ρ_p/ρ_f
τ = dimensionless time, $\alpha_b t/(r_i^+ r_p^+ Ra^{*1/4})$
ξ = volumetric phase fraction in a particle

Subscripts

b = bulk fluid
bf = bulk-to-fluid ratio
c = cooled section
f = suspending fluid
h = heated section or heat transfer coefficient
ℓ = liquid phase of PCM
lat = latent heat
m = melting point or mean quantity
p = particle
pf = particle-to-fluid ratio
s = solid phase of PCM
sen = sensible heat
w = pipe wall

Superscripts

$-$ = surface-averaged quantity
$*$ = ratio of quantities
$+$ = dimensional quantity

Introduction

Natural circulation (thermosyphon) loops of various configurations and operating conditions have been the subject of study of numerous investigations due to their wide ranges of technological applications, such as nuclear reactor emergency cooling system, solar heating and cooling systems, geothermal energy generation, waste heat recovery system, turbine blade cooling, and electronic cooling. In the natural circulation loop, the fluid flow driven by thermally induced density gradient dissipates heat from a heated section and transports to a higher elevation cooled section, which can serve as a low-cost and highly reliable passive heat transfer device. The behavior of natural circulation loop is controlled by interaction between buoyancy and friction forces. Comprehensive literature reviews on modeling and simulations, system stability, experimental studies of the natural circulation loops can be found in the papers by Japikse (1973), Zvirin (1982) and Greif (1988). Compared to single-phase systems, two-phase natural circulation loops not only are capable of generating larger buoyancy force, but also utilize latent heat transport associated with phase change of liquid contained in the loop, thereby resulting in higher heat transfer rates.

Incorporating technologies of microencapsulation and emulsion, an effective heat transfer enhancement medium has been proposed by Hart and Thornton (1982) that fine solid-liquid phase-change material (PCM) particles (typically with diameter of 1-20 μm) are dispersed in a carrier or suspending fluid (PCM slurries or suspensions). The PCM suspension flow can serve as a dual-functional medium for sensible and/or latent heat transport. The efficacy of heat transfer enhancement of using the PCM suspensions has been fully demonstrated for the forced convection in duct flows (Sohn and Chen, 1985; Charunyakorn *et al.*, 1991; Goel *et al.*, 1994; Choi *et al.*, 1994; Zhang and Faghri, 1995; Choi and Choi, 2000; Ho *et al.*, 2004). By contrast, limited studies have been reported concerning heat transfer enhancement using the PCM suspensions in the buoyancy-driven convection configurations. Katz (1976) conducted an experimental investigation of natural convection heat transfer in a cubic enclosure heated from below using rather large PCM capsules. The experimental results in the turbulent regime showed a 100 percent heat transfer enhancement. Datta *et al.* (1992) reported experimental results for natural convection heat transfer in a similar cubic enclosure using microencapsulated PCM suspensions. The heat transfer rate was found to augment about 80 percent for the concentration below 5 percent. It is only recently that Harhira *et al.* (1996) developed a numerical study for buoyancy-driven boundary layer flow of PCM suspensions along a vertical plate. Boundary layer approximations of continuum equations for the conservation of mass, momentum, energy, and species for binary mixture of dispersed particles in a continuous fluid have been developed. The heat transfer model adopted for phase-change process in the particles appears restricted with the assumption of neglecting transverse motion of the particles.

In the present paper, we aim to explore feasibility of incorporating the PCM suspensions as the heat transfer enhancement medium in a natural circulation loop, which has not been examined previously. To this end, heat transfer characteristics of a simple rectangular recirculation loop containing the PCM suspensions as shown schematically in Figure 1 are numerically investigated using a 2D formulation with an approximate enthalpy model to describe the solid-liquid phase-change process of the particles.

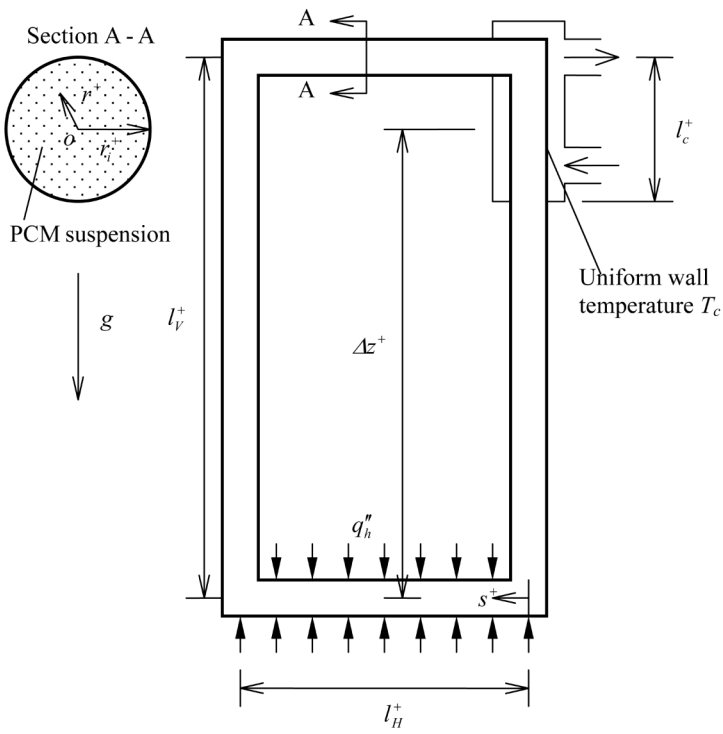

Figure 1.
Schematic diagram of rectangular thermosyphon loop and coordinate system

Source: Ho *et al.*

Problem formulation

The rectangular natural circulation loop considered, as shown in Figure 1, is constructed of circular pipe of inner radius r_i^+ and filled with s suspension fluid. The loop is heated uniformly by a constant heat flux q_{h}'' over the bottom horizontal leg $\left(l_{\mathrm{h}}^+ = l_{\mathrm{H}}^+\right)$ and cooled isothermally over a length l_{c}^+ of the upper portion of the right vertical leg at a constant temperature T_{c}; while the rest of the loop is assumed thermally insulated. In the mixture continuum formulation adopted for the buoyancy-driven circulation flow of the PCM suspensions, the simplifying assumptions adopted are as follows:

(1) the particles are rigid spheres of homogeneous size that is sufficiently small compared with the characteristic dimension of flow;

(2) the mixture is dilute, homogenous with a volumetric particle concentration c_{v} and is considered as Newtonian fluid;

(3) the dispersed particles are neutrally buoyant in the mixture;

(4) the flow is assumed to be laminar and in the axial direction only, which can vary axisymmetrically in the radial direction;

(5) local thermodynamic equilibrium is assumed except during the solid-liquid phase-change process of particle;

(6) the melting/freezing of the particles takes place at a fixed fusion temperature;
(7) density change associated with the solid-liquid phase change in the particles is negligible;
(8) all physical properties of the mixture are constant invoking the Boussinesq approximation;
(9) effect of curvature of the loop is negligibly small; and
(10) viscous dissipation in the flow is neglected.

Based on the foregoing assumptions, the dimensionless governing equations for the conservations of mass, momentum and energy for the present problem are the following.

Continuity equation:

$$\frac{\partial u}{\partial s} = 0. \tag{1}$$

Momentum equation integrated over the entire length of the loop:

$$\frac{1}{\mathrm{Pr}\,\mathrm{Ra}^{*1/4} r_{\mathrm{p}}} \frac{\partial u}{\partial \tau} = \frac{1}{r}\frac{\partial}{\partial r}\left(r\frac{\partial u}{\partial r}\right) + \frac{(\mathrm{Ra}^{*1/4} R_{\mathrm{L}})^3}{\gamma_{\mathrm{L}} l_{\mathrm{L}}} \int_0^{l_{\mathrm{L}}} \theta \phi \, \mathrm{d}s, \tag{2}$$

where $\phi = 1$ for $l_{\mathrm{H}} < s < (l_{\mathrm{L}}/2)$, $\phi = -1$ for $(l_{\mathrm{L}}/2 + l_{\mathrm{H}}) < s < l_{\mathrm{L}}$, and $\phi = 0$ for $0 \le s \le l_{\mathrm{H}}$ or $(l_{\mathrm{L}}/2) < s < (2l_{\mathrm{H}} + l_{\mathrm{v}})$. The foregoing dimensionless axial lengths of the rectangular loop can be expressed in terms of the aspect ratio of the loop AR and the mean relative elevation of the cooled section to the heated section Δz as follows: $l_{\mathrm{L}} = (1 + 2\Delta z)(1 + \mathrm{AR})$, $l_{\mathrm{H}} = (1 + 2\Delta z)(\mathrm{AR}/2)$, and $l_{\mathrm{v}} = (1 + 2\Delta z)/2$. Moreover, the correction factor of loop length $\gamma_{\mathrm{L}} (\ge 1)$ is introduced in the buoyancy force term of equation (2) to account for the minor losses of the loop (Huang and Zelaya, 1988).

Energy equation:

$$\begin{aligned}\left(\frac{1}{R_{\mathrm{L}} l_{\mathrm{L}} r_{\mathrm{p}}}\right)\frac{\partial \theta}{\partial \tau} + u\frac{\partial \theta}{\partial s} &= \left(\frac{R_{\mathrm{L}} l_{\mathrm{L}}}{\mathrm{Ra}^{*1/4}}\right)\left[\frac{\partial^2 \theta}{\partial s^2} + \frac{1}{(R_{\mathrm{L}} l_{\mathrm{L}})^2}\left(\frac{\partial^2 \theta}{\partial r^2} + \frac{1}{r}\frac{\partial \theta}{\partial r}\right)\right] \\ &- \left(\frac{\rho^*_{\mathrm{pf}}}{\rho^*_{\mathrm{bf}}}\right)\frac{c_{\mathrm{v}}}{\mathrm{Ste}^*}\left[\left(\frac{1}{R_{\mathrm{L}} l_{\mathrm{L}} r_{\mathrm{p}}}\right)\frac{\partial \xi_\ell}{\partial \tau} + u\frac{\partial \xi_\ell}{\partial s}\right].\end{aligned} \tag{3}$$

The last two terms on the right-hand side of equation (3) account for the transport of latent heat absorption/release associated with the melting/freezing of the PCM particles, in which closure for the liquid-phase volume fraction of the particles ξ_ℓ is required. An approximate enthalpy model developed in the earlier study (Ho *et al.*, 2004) was adopted here to describe the phase-changing process in the PCM particles, which can be expressed in a dimensionless formulation as:

$$\left(\frac{1}{R_{\mathrm{L}} l_{\mathrm{L}} r_{\mathrm{p}}}\right)\frac{\partial \xi_\ell}{\partial \tau} + u\frac{\partial \xi_\ell}{\partial s} = \left(\frac{3\mathrm{Bi}_{\mathrm{p}}}{r_{\mathrm{p}}^2}\right)\left(\frac{k^*_{\mathrm{pf}}}{k^*_{\mathrm{bf}}}\right)\left(\frac{\rho^*_{\mathrm{bf}}}{\rho^*_{\mathrm{pf}}}\right)\left(\frac{\mathrm{Ste}^*}{R_{\mathrm{L}} l_{\mathrm{L}} \mathrm{Ra}^{*1/4}}\right)\theta. \tag{4}$$

The relevant boundary conditions of the problem are summarized as follows:

$$\frac{\partial \theta}{\partial r} = 1, \;\; u = 0; \quad r = 1, \;\; 0 \le s \le l_{\mathrm{h}}, \tag{5a}$$

$$\frac{\partial \theta}{\partial r} = 0, \;\; u = 0; \quad r = 1, \;\; l_{\mathrm{h}} \le s \le (2l_{\mathrm{H}} + l_{\mathrm{v}}) \;\; \text{or} \;\; (2l_{\mathrm{H}} + l_{\mathrm{v}} + 1) \le s \le l_{\mathrm{L}}, \tag{5b}$$

$$\theta = -\mathrm{Sb}^*, \;\; u = 0; \quad r = 1, \;\; (2l_{\mathrm{H}} + l_{\mathrm{v}}) \le s \le (2l_{\mathrm{H}} + l_{\mathrm{v}} + 1), \tag{5c}$$

$$\frac{\partial \theta}{\partial r} = 0, \;\; \frac{\partial u}{\partial r} = 0, \quad r = 0, \;\; 0 \le s \le l_{\mathrm{L}}. \tag{5d}$$

From the foregoing it is evident that a parametric study of the steady-state heat transfer characteristics of the suspension-filled natural circulation loop considered involves the following dimensionless parameters: the modified Rayleigh number, Ra*; the modified Stefan number, Ste*; the modified subcooling factor Sb*; the dimensionless length of the heated section, l_{h}; the mean relative elevation between the cooled and heated sections Δz; the aspect ratio of the rectangular loop, AR; the volumetric concentration of PCM particles, c_{v}; the dimensionless pipe radius, R_{L}; the dimensionless particle radius, r_{p}; and the property ratios, k^*_{pf}, ρ^*_{pf}. Moreover, the particle Biot number, Bi_{p}, and the property ratios, k^*_{bf} and ρ^*_{bf}, that also appear in the above formulation are evaluated adopting the relationships given by Charunyakorn *et al.* (1991).

Furthermore, several quantities of interest that can be derived from the solution of the foregoing governing differential equations of the problem are defined in dimensionless form as discussed below.

Local mean velocity and bulk temperature of the suspension fluid, u_{m} and θ_{b}, as well as the mean liquid-phase fraction of PCM particles, ξ_{b}, at a given cross section of the loop are, respectively, calculated from

$$u_{\mathrm{m}} = 2\int_0^1 u(r) r \, \mathrm{d}r, \tag{6}$$

$$\theta_{\mathrm{b}}(s) = \frac{\displaystyle\int_0^1 u\theta(r,s) r \, \mathrm{d}r}{\displaystyle\int_0^1 ur \, \mathrm{d}r}, \tag{7}$$

$$\xi_{\mathrm{b}}(s) = \frac{\displaystyle\int_0^1 u\xi_{\ell}(r,s) r \, \mathrm{d}r}{\displaystyle\int_0^1 ur \, \mathrm{d}r}. \tag{8}$$

Local dimensionless heat flux at the isothermally cooled section is presented by the local Nusselt number Nu_{c}, which is defined as

$$\mathrm{Nu_c} = \frac{2\left(\frac{\partial\theta}{\partial r}\right)_{r=1}}{\theta_w - \theta_b}. \tag{9}$$

If the axial fluid conduction is assumed negligible, the total heat transfer rate by the steady-state suspension flow over a given loop length between $s = s_1$ and s_2 can be derived based on an integral energy balance and takes the form

$$\begin{aligned} q^*_{1-2} &= \frac{1}{l_h}\int_{s_1}^{s_2}\left(\frac{\partial\theta}{\partial r}\right)_{r=1}\mathrm{d}s \\ &\approx \frac{u_m}{2}(\mathrm{Ra}^{*1/4}R_L)\left(\frac{l_L}{l_h}\right) \\ &\times\left\{[\theta_b(s=s_2)-\theta_b(s=s_1)] + \left(\frac{\rho^*_{pf}}{\rho^*_{bf}}\right)\left(\frac{c_v}{\mathrm{Ste}^*}\right)[\xi_b(s=s_2)-\xi_b(s=s_1)]\right\}. \end{aligned} \tag{10}$$

Equation (10) appears to relate the bulk mean temperature of suspension fluid θ_b, as well as the mean liquid-phase fraction of PCM particles ξ_b with the total convection heat transfer rate q^*_{1-2}. Specifically, equation (10) reveals that the convection heat transfer by the PCM suspension flow in the loop may be due to transport of sensible heat, as well as of latent heat, which are denoted by the following expressions, respectively.

$$(q^*_{1-2})_{sen} = \frac{u_m}{2}(\mathrm{Ra}^{*1/4}R_L)\left(\frac{l_L}{l_h}\right)[\theta_b(s=s_2)-\theta_b(s=s_1)], \tag{11}$$

and

$$(q^*_{1-2})_{lat} = \frac{u_m}{2}\left(\mathrm{Ra}^{*1/4}R_L\right)\left(\frac{l_L}{l_h}\right)\left(\frac{\rho^*_{pf}}{\rho^*_{bf}}\right)\left(\frac{c_v}{\mathrm{Ste}^*}\right)[(\xi_b(s=s_2)-\xi_b(s=s_1)]. \tag{12}$$

Furthermore, to quantify efficacy of the PCM suspension as a heat transfer enhancement medium, effectiveness of the maximum temperature control, $\varepsilon_{T_{max}}$, at the heated section and of the averaged heat transfer enhancement, ε_h, at the cooled section of the circulation loop are, respectively, defined as follows:

$$\varepsilon_{T_{max}} = (\theta_{w,h,max,f}/\theta_{w,h,max,b})(k^*_{bf}) = (T_{w,h,max,f}-T_m)/(T_{w,h,max,b}-T_m), \tag{13}$$

$$\varepsilon_h = (\overline{\mathrm{Nu}}_{c,b}/\overline{\mathrm{Nu}}_{c,f})(k^*_{bf}) = \bar{h}_{c,b}/\bar{h}_{c,f}. \tag{14}$$

Numerical method

Spatial discretization of the differential equations is performed on a uniform mesh laid over the loop, incorporating the second-order central difference scheme for the diffusion terms and the QUICK scheme (Leonard, 1979) for the convective terms. Temporal derivative terms in the differential equations are treated using an implicit approximation with second-order accuracy. Steady-state solutions to the governing equations of the problem are obtained numerically by a pseudo-transient approach. The steady-state temperature and velocity fields are considered convergent when the

maximum variation between the values of computed at the present and previous iterations is less than 10^{-5}. All computations were performed with double-precision arithmetic. In addition, an energy balance was checked for each converged simulation to ensure that difference of the total heat transferred through the isothermal cooled section from the total heat input through the heated section is less than 0.1 percent.

To verify the present formulation and numerical method adopted, simulations have been performed for selected cases of a 2D circulation flow and heat transfer in a single-phase toroidal loop to compare with results presented in the paper (Metrol *et al.*, 1982). An excellent agreement was found. In order to ensure the grid convergence of the numerical results, different grids have been tested. Simulation results shown later have been obtained for several mesh ranging from 101 (radial direction) $\times$ 2001 (axial direction) to 201×3001, depending mainly on the modified Rayleigh number Ra*, the concentration c_v, and the modified Stefan number Ste*.

Results and discussion

Numerical simulations have been undertaken to unveil parametric dependence of the steady-state heat transfer characteristics of the suspension-filled circulation loop on the modified Rayleigh number Ra*, the modified Stefan number Ste*, the particle fraction c_v, and the modified subcooling factor Sb* in the following ranges: $Ra^* = 10^9$-10^{13}, $Ste^* = 0.05$-0.5, $c_v = 0$-20 percent, $Sb^* = 0$-2.0. The remaining parameters pertinent to the circulation loop are held constant as follows: $k^*_{pf} = 0.412$, $\rho^*_{pf} = 0.774$, $r_p = 0.023$, $R_L = 4.35 \times 10^{-3}$, AR = 1, and $\Delta z = 2.0$.

Induced flow field

First of all, Figure 2 shows the steady-state velocity profiles at various modified Rayleigh numbers, respectively, for the suspension with a volume fraction of the PCM particles $c_v = 10$ percent at $Ste^* = 0.1$ and $Sb^* = 0.6$. Also included in the figure is the corresponding velocity profiles of the pure suspending fluid (c_v=0 percent) for comparison. As can be expected, with the increasing Ra* beyond a certain value the increasingly enhanced buoyancy-driven flow of the suspension or the pure fluid features a shift of the location of the maximum velocity away from the axis towards the wall of the loop. Moreover, the magnitude of the dimensionless velocity of the suspension appears to be increasingly smaller than that of pure fluid with increasing Ra*.

In Figure 3 the Reynolds number of the buoyancy-driven flow, which is proportional to the mass flow rate induced in the circulation loop, is plotted as a function of the modified Rayleigh number for the suspension of various particle fractions c_v with $Ste^* = 0.1$ and $Sb^* = 0.6$. Consistent with the results shown in Figure 2, the induced Reynolds number generally increases as the modified Rayleigh number is increased. The opposite is true for an increase of the particle fraction. At $Ra^* = 10^{11}$, for instance, an increase of c_v up to 15 percent yields a reduction of more than 50 percent for the magnitude of Re, as shown in Figure 3. In effect, a reduction of the Reynolds number, or equivalently the circulation flow rate, causes prolongation of the PCM particle residence time through and meanwhile may significantly degrade the convective heat transfer over the heated/cooled sections of the loop. Such competing effects play vital roles for the progress of the phase-change processes of the PCM particles in the circulation loop.

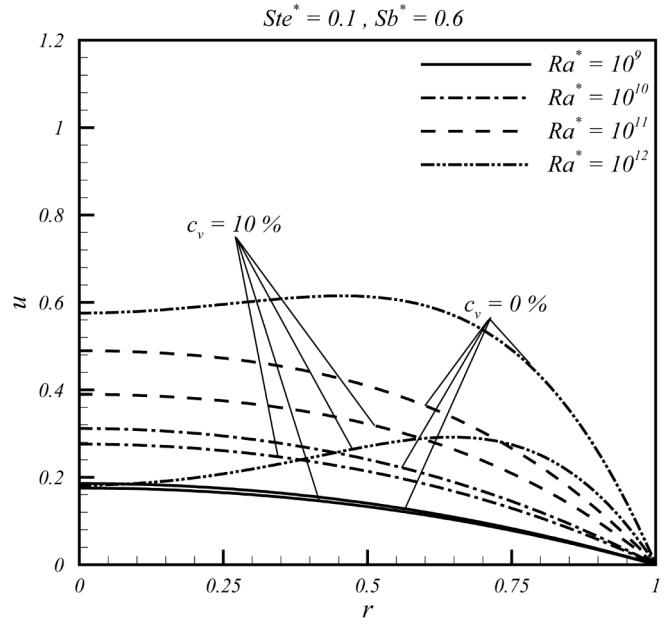

Source: Ho *et al.*

Figure 2.
Velocity profiles for various modified Rayleigh numbers under Ste* = 0.1, Sb* = 0.6, and c_v=0 and 10 percent

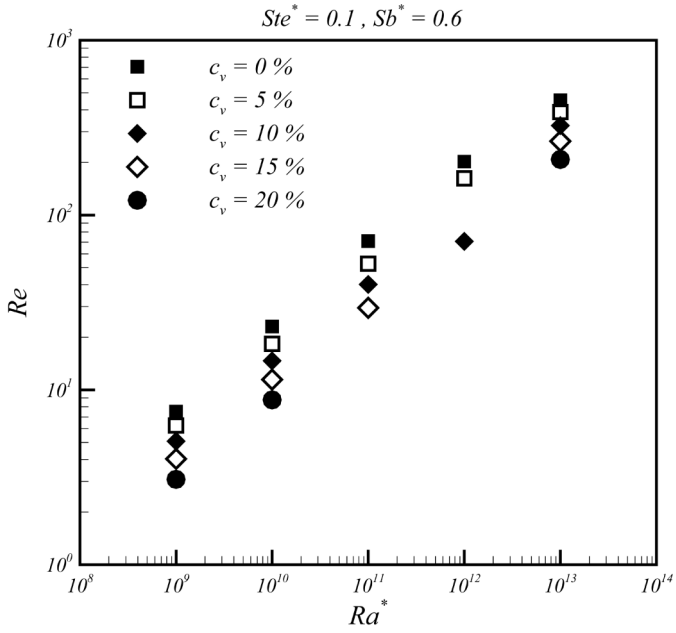

Source: Ho *et al.*

Figure 3.
Relation of Reynolds number with the modified Rayleigh number for various concentration under Ste* = 0.1, and Sb* = 0.06

Furthermore, the dependence of the Reynolds number on the modified Stefan number and the modified subcooling factor of the suspension is illustrated in Table I for c_v=10 percent. An overview of the table indicates that the influence of the modified Stefan number or the modified subcooling factor is a function of the modified Rayleigh number. An increase of Ste*/Sb* produces, respectively, a monotonic increase/decrease of Re for Ra* = 10^{10}; while a non-linear variation of Re for the higher Ra* of 10^{12}, suggesting occurrence of a minimum flow rate over the range of Ste*/Sb* considered. Specifically, as shown in Table I, for Ra* = 10^{12} the suspension with Ste* = 0.1 has a lower Reynolds number and hence a longer residence time for the particle phase-change processes in the loop, leading to higher contribution of latent heat transport as will be shown in the later sections.

Axial distributions of temperature and particle liquid fraction

Next, the axial distributions of the wall temperature, θ_w, the bulk temperature, θ_b, and the mean liquid fraction of particles, ξ_b are examined to gain basic understanding of steady-state thermal behavior of the suspension-filled circulation loop. Figure 4 shows the results for the suspension loop of c_v=10\hskip2pt percent with Ste* = 0.1 and Sb* = 0.6 together with the corresponding results of the pure fluid loop under various modified Rayleigh numbers. Over the heated section of iso-flux, as can be seen in Figures 4(a) and (b), both the wall and bulk temperatures for the pure fluid loop display a linear increase but at decreasing slope with increasing Ra*, leading to increasingly smaller temperature rise. In contrast, the temperature rise over the heated section of the suspension loop is closely interrelated with melting behavior of the PCM particles as shown by the curves of the mean liquid fraction ξ_b in Figure 4(c). The suspension entering the heated section may be subcooled (below the particle fusion temperature) with fully frozen particles, depending primarily on the freezing process undergone previously in the cooled section. From the inlet of the heated section, a rather non-linear temperature increase at a smaller slope prevails on the wall through an axial distance over which the melting process of the particles is under way, indicative of the temperature reduction capability due to latent heat absorption involved with the particle melting. Beyond an axial location where the particles become fully melted and so the slopes for the wall and bulk temperatures change, as can be detected in Figure 4 for Ra* = 10^{10} and 10^{11}; the suspension starts to act like a pure fluid exhibiting a linear rising trend of temperature till the heated section outlet. With further increase of Ra* up to 10^{12}, the intensified circulation flow and the enhanced convective transport of sensible heat gives rise to considerable reductions in the residence time of the particles, as well as the wall temperature over the heated section, respectively.

Table I.
Dependence of Reynolds number and friction factor on the modified Stefan number and modified subcooling factor for c_v=10 percent

		Re			
Ra*	Ste*	Sb* = 0	Sb* = 0.6	Sb* = 1.0	Sb* = 2.0
10^{10}	0.05		13.52		
	0.1	16.47	14.66	14.02	13.70
	0.5		16.02		
10^{12}	0.05		84.03		
	0.1	141.4	70.73	144.2	144.6
	0.5		114.0		

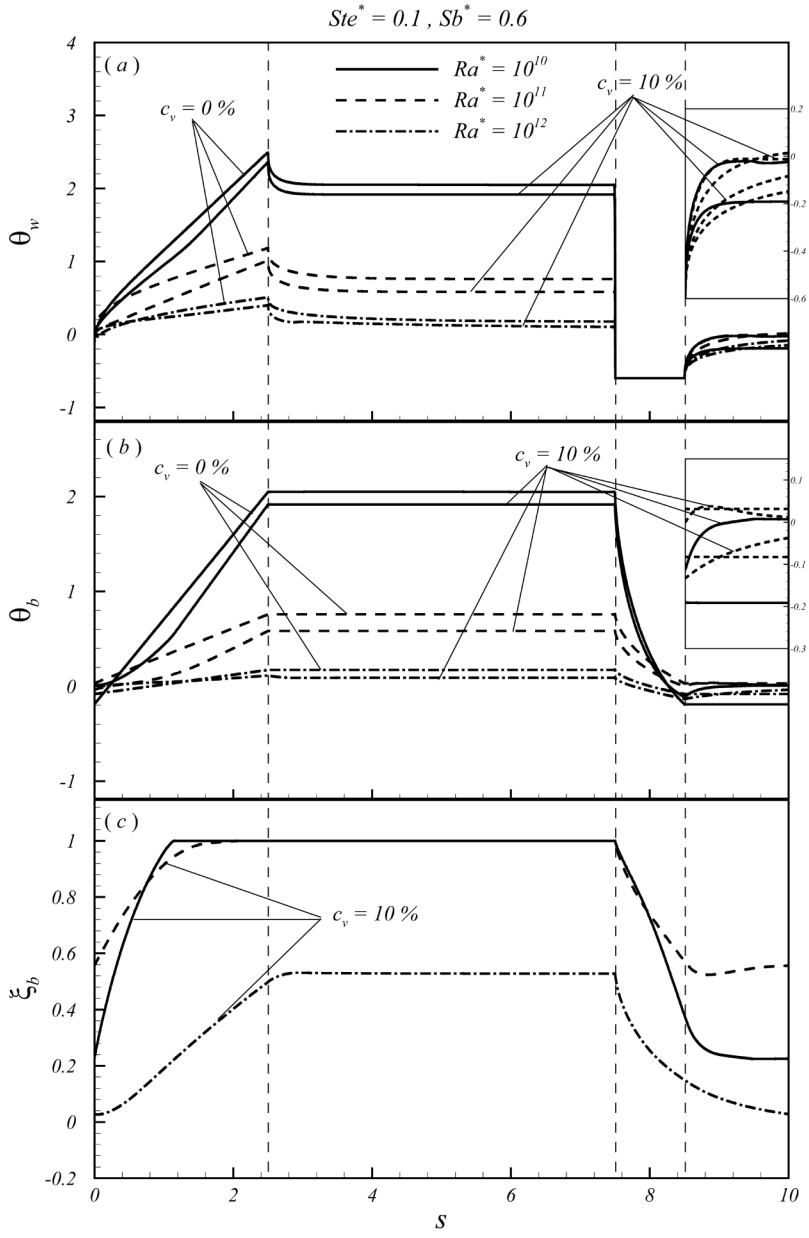

Source: Ho *et al.*

Figure 4.
Axial distributions of (a) the dimensionless wall temperature θ_w, (b) the mean fluid temperature θ_b, and (c) the mean liquid fraction of PCM suspension ξ_b for various modified Rayleigh numbers under Ste* = 0.1, Sb* = 0.6, and $c_v = 0$ and 10 percent

Consequently, the particle melting is significantly retarded, resulting in the partially melted particles at the exit of the heated section as shown in Figure 4(c). Along the adiabatic section following the heated section, the wall temperature, as well as the bulk temperature remain essentially unchanged and hence so does the mean phase fraction of the suspension.

Next, the suspension reaching the cooled section may be highly superheated (above the particle fusion temperature) if the particles are already fully melted before reaching the heated section outlet as shown in Figure 4(c) for $Ra^* = 10^{10}$ and 10^{11}. The heat extracted through the isothermally cooled section is then partly due to sensible cooling of the superheated suspension down to the particle fusion temperature. Resembling to that found for the melting process in the heated section, the extent of particle freezing at the cooled section outlet is markedly degraded with the increase of Ra*. Finally, over the adiabatic section approaching the heated section, the wall temperature may remain substantially subcooled that the partially frozen particles out of the cooled section further proceed to solidify. At the inlet of the heated section, the returning suspension could be substantially subcooled, which would in turn impede the subsequent melting process. To sum up, the melting/freezing processes in the heated/cooled sections are interrelated closely in the mutual bearing on the thermal conditions (subcooled/superheated temperature, particle phase fraction) of their inlet suspension.

In what follows, the attention will be focused on the effects of the particle fraction c_v, the modified Stefan number Ste*, and the modified subcooling factor Sb* on the distributions of θ_w, θ_b, and ξ_b, which are, respectively, a strong function of the modified Rayleigh number.

An inspection of Figures 5 and 6 shows that the effect of increasing particle fraction may appear qualitatively similar/opposite to that of decreasing modified Stefan number, depending on the modified Rayleigh number. For $Ra^* = 10^{10}$ the melting process of the suspension with higher particle fraction/lower modified Stefan number proceeds over a longer axial distance, resulting in markedly lower wall and bulk temperatures over the heated section. Over the cooled section, the freezing process of the suspension with higher particle fraction/lower modified Stefan number produces lower frozen fraction at the cooled section outlet, as well as at the heated section inlet, mainly due to degradation of convective sensible heat transfer associated with the reduced circulation flow. By contrast, at the higher modified Rayleigh number of 10^{12}, the influence of varying c_v/Ste* on the wall and bulk temperature profiles over the loop is drastically degraded; the inlet suspension for the heated or cooled section appears slightly subcooled or superheated, as shown in Figures 5(c) and 6(c). As shown in Figure 3 and Table I, under the condition of $Ra^* = 10^{12}$, a substantially reduced circulation flow rate prolonging residence time arises with an increase of the particle fraction up to 10 percent; while a greatly enhanced flow rate augmenting the convective heat transfer with an increase of the modified Stefan number to 0.5. Accordingly, the melting/freezing processes are greatly promoted.

Next, the influence of the modified subcooling factor is shown in Figure 7 for two different values of Ra* at $Ste^* = 0.1$ and $c_v = 10$ percent. Note that a positive value of the modified subcooling factor in effect specifies the extent of the cooled wall temperature below the particle fusion temperature. There appears two extreme scenarios shown in Figure 7. The first extreme scenario occurs under the condition of $Sb^* = 0$, for which the cooled wall is maintained at the particle fusion temperature.

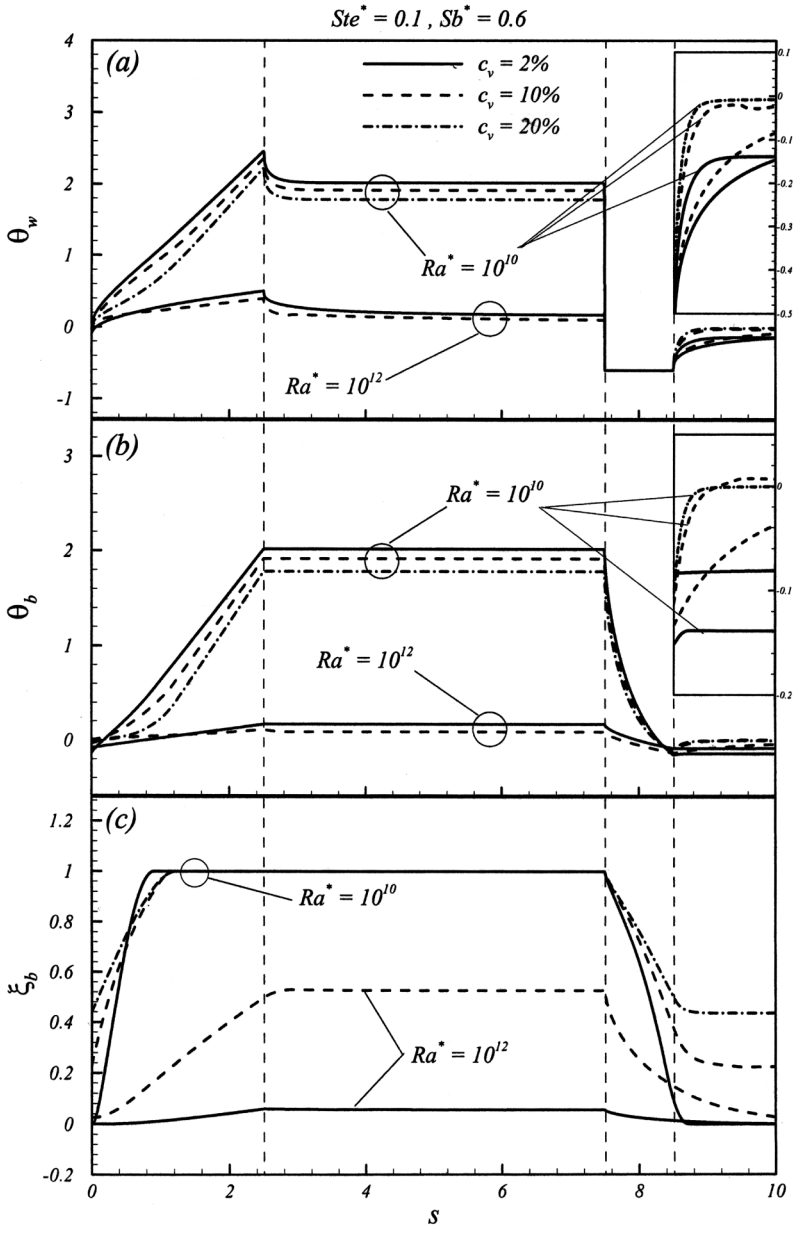

Source: Ho *et al.*

Figure 5.
Axial distributions of (a) the dimensionless wall temperature θ_w, (b) the mean fluid temperature θ_b, and (c) the mean liquid fraction of PCM suspension ξ_b for various concentrations under Ste* = 0.1, Sb* = 0.6, and Ra* = 10^{10} and 10^{12}

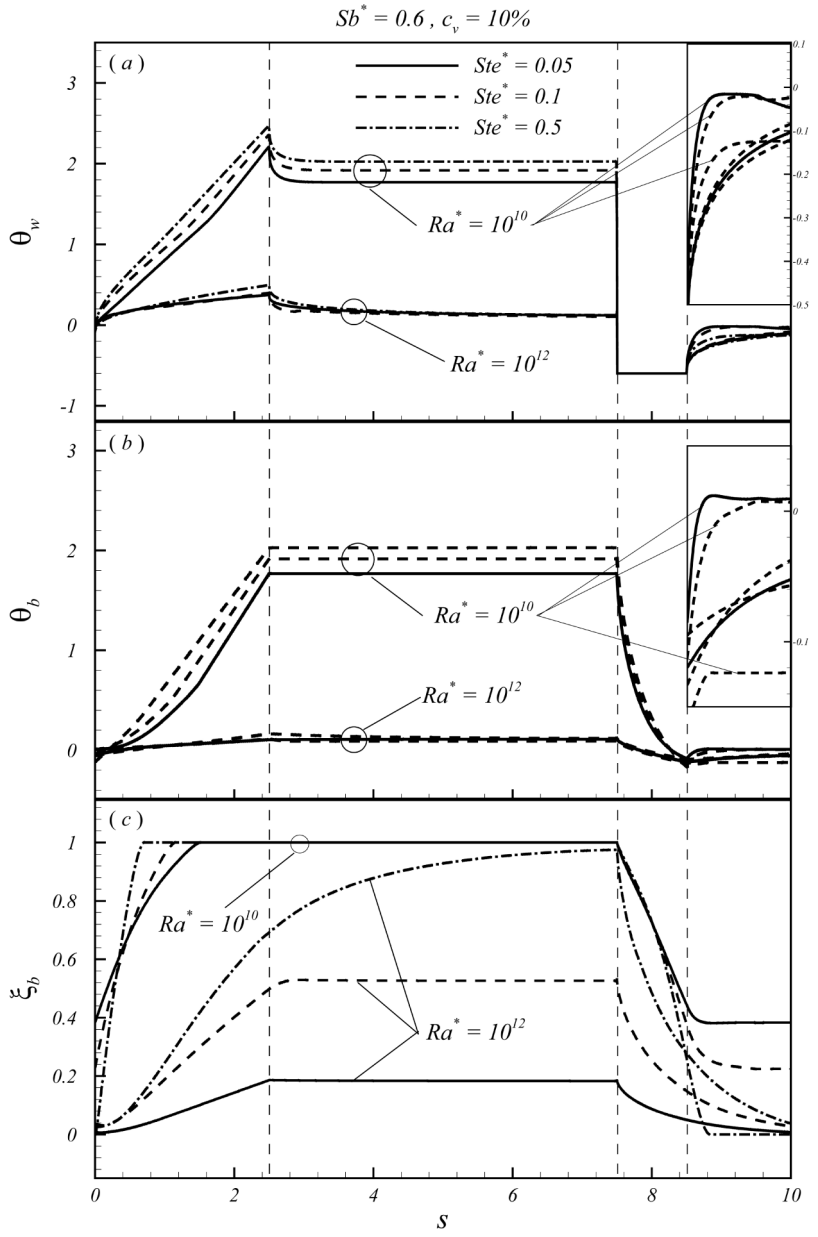

Figure 6.
Axial distributions of (a) the dimensionless wall temperature θ_w, (b) the mean fluid temperature θ_b, and (c) the mean liquid fraction of PCM suspension ξ_b for various modified Stefan numbers under Sb* = 0.6, c_v=10 percent, and Ra* = 10^{10} and 10^{12}

Source: Ho *et al.*

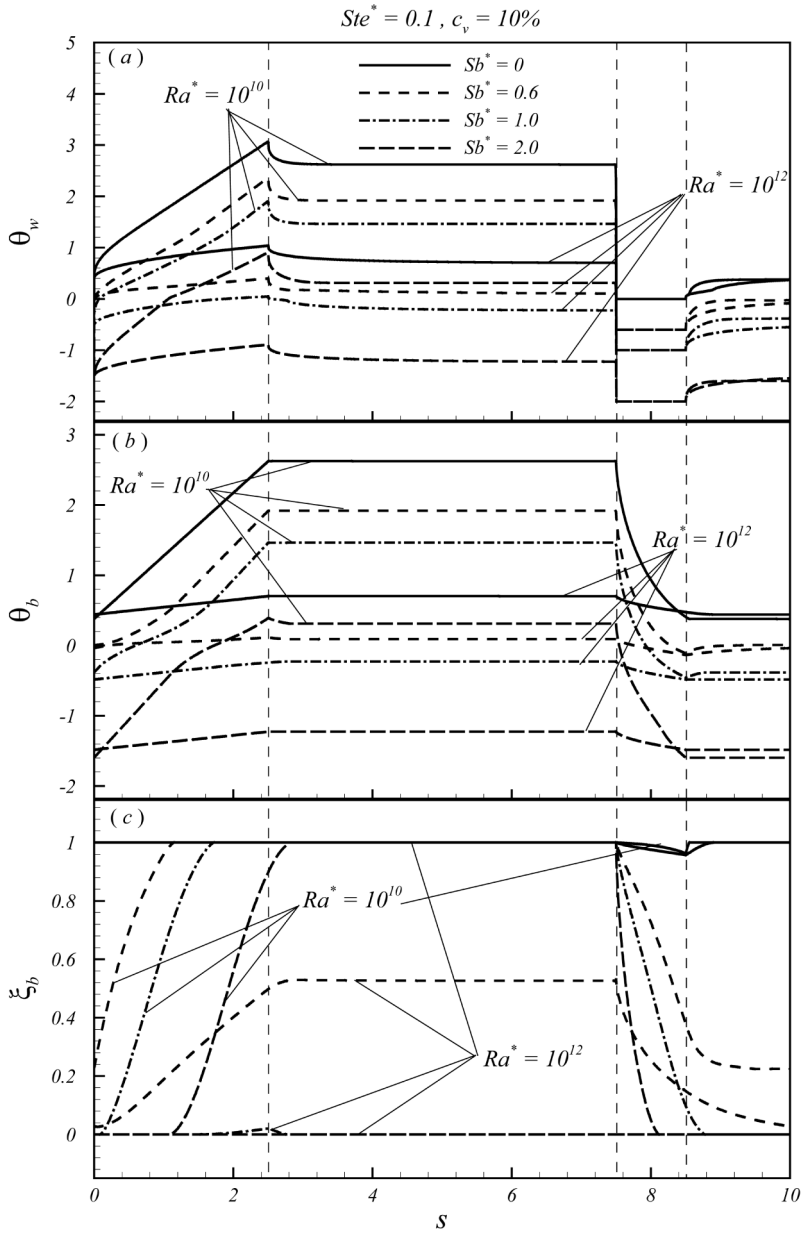

Source: Ho *et al*.

Figure 7.
Axial distributions of (a) the dimensionless wall temperature θ_w, (b) the mean fluid temperature θ_b, and (c) the mean liquid fraction of PCM suspension ξ_b for various modified subcooling factors under Ste*=0.1, c_v=10 percent, and Ra* = 10^{10} and 10^{12}

The particles appear fully melted throughout the loop except the region around the cooled section where the particles are slightly frozen. An axial distribution similar to that found for the pure fluid prevails for the wall and bulk temperatures of the suspension-filled loop. With a subcooled wall temperature over the cooled section ($Sb^* > 0$), the particle freezing process as expected is markedly promoted. At $Sb^* = 1$, the particles become fully frozen within the cooled section at lower modified Rayleigh number of 10^{10} as shown in Figure 7(c). On the other hand, the subcooled suspension out of the cooled section with increasing Sb* tends to impede increasingly the subsequent melting process over the heated section. As shown in Figure 7, under the condition of $Sb^* = 2$ with $Ra^* = 10^{10}$, with the highly subcooled suspension returning to the heated section, the wall temperature appears to remain subcooled over a substantial distance from the inlet of the heated section. As a result, the axial location where the melting process initiates shifts far downward from the heated section inlet. As the modified Rayleigh number is increased, the effect of the modified subcooling factor becomes further distinctive. At the higher $Ra^*(= 10^{12})$, an increase of Sb* up to 2 leads to another extreme scenario opposite to the afore-described for $Sb^* = 0$. The melting process appears completely suppressed over the heated section except the region near the outlet. The foregoing clearly implies that controlling of the cooled wall temperature at a proper degree of subcooling is vital to sustain the freezing/melting processes of the particles in the loop.

Another quantity of technical interest in the aspect of wall temperature control at the heated section of iso-flux is the dimensionless maximum wall temperature, $\theta_{w,h,max}$, which is presented as a function of the modified Rayleigh number for various particle fractions in Figure 8. In comparison with the results for the pure fluid also shown in Figure 8, it is evident that for a fixed Ra*, the maximum heated wall temperature $\theta_{w,h,max}$ drops as the particle fraction is increased. Such effect of temperature reduction with an increase of particle fraction, however, tends to degrade gradually with an increase of the modified Rayleigh number. At $Ra^*(= 10^{13})$, as can be seen in Figure 8, the maximum heated-wall temperature appears insensitive to variation of the particle fraction, indicative of negligible latent heat effect due to the particle melting over the heated section.

Heat transfer performance

The heat transfer characteristics at the isothermally cooled wall are shown in Figure 9 where the averaged Nusselt number $\overline{Nu}_c$ is plotted against the modified Rayleigh number. The suspension with increasing particle fraction clearly has increasingly higher $\overline{Nu}_c$ than that of pure fluid, reflecting the effect of latent heat release associated with the particle freezing. For $Ra^* = 10^{11}$, for instance, an increase of the particle fraction to 15 percent gives an increase in $\overline{Nu}_c$ of more than 17 percent above that of the pure fluid. This beneficial effect due to an increase of the particle fraction appears degraded at higher or lower Ra*. At $Ra^* = 10^{13}$, in the absence of latent heat transport involved with the particle freezing, the average Nusselt number remains invariant with variation of the particle fraction.

The thermal efficacy of the PCM suspension is quantitatively assessed in terms of the maximum wall temperature control effectiveness $\varepsilon_{T_{max}}$ (equation (13)) and the averaged heat transfer effectiveness ε_h (equation (14)), respectively, over the heated and cooled sections of the circulation loop. The effectiveness parameters $\varepsilon_{T_{max}}$ and ε_h

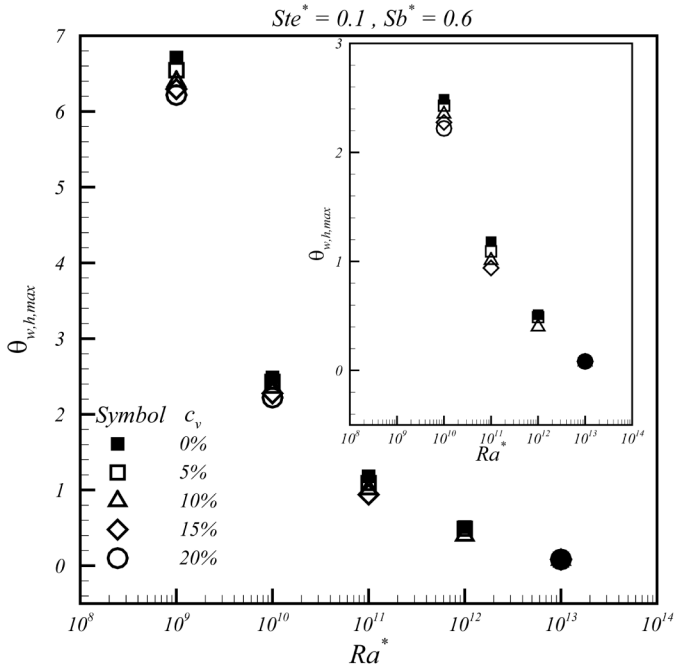

Source: Ho *et al.*

Figure 8.
Relation of the maximum wall temperature $\theta_{w,h,max}$ at the heated section with the modified Rayleigh number for various particle fractions under Ste* = 0.1, Sb* = 0.6

are found to depend significantly on the modified Rayleigh number, the particle fraction, the modified Stefan number, and the modified subcooling factor, as shown in Figure 10 and Table II. Under a fixed particle fraction, a non-monotonic variation of $\varepsilon_{T_{max}}$ or ε_h with respect to Ra*, Ste* or Sb* can be observed, suggesting existence of a local maximum effectiveness in the parameter ranges considered. For instance, as can be discerned in Table II, under the condition of c_v=10 percent and Ra* = 10^{12} the temperature control effectiveness $\varepsilon_{T_{max}}$ at the heated section displays a maximum value of 2.310 at Sb* = 1. Also can be observed in Figure 10 for the suspension with fixed particle fraction of 10 percent, the variations of the effectiveness parameters $\varepsilon_{T_{max}}$ and ε_h display a local maximum value, respectively, at Ra* = 10^{12} and 10^{11}. Moreover, the particle fraction can affect the effectiveness parameters $\varepsilon_{T_{max}}$ and ε_h differently, depending on the modified Rayleigh number. For Ra* = 10^{11}-10^{12}, an increase of the particle fraction further promotes the effectiveness parameters to be increasingly greater than unity. For the modified Rayleigh number outside the range, the opposite is true that the effectiveness parameters become increasingly less than unity. The foregoing, in consistent with the observations made previously, implies that there exists a flow regime in the parameter domain where the beneficial effects of using the PCM suspension to enhance the heat transfer in the circulation loop could be obtainable.

Finally, the contribution of latent heat transport to the overall heat transfer in the heated/cooled sections of the circulation loop is presented in terms of $(q^*_h)_{lat}$ and $(q^*_c)_{lat}$, as shown in Figure 11 and tabulated in Table III. An overview of the Figure 11

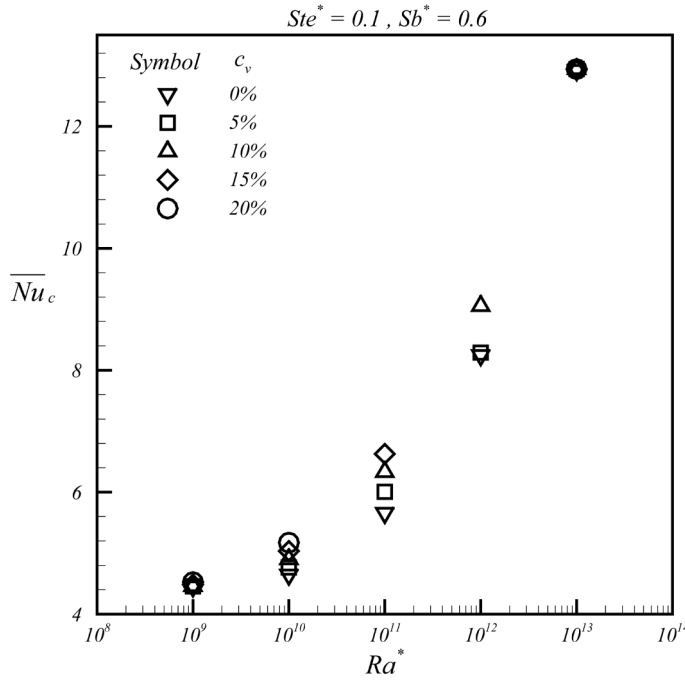

Figure 9.
Relation of the averaged Nusselt number $\overline{Nu}_c$ at the cooled section with the modified Rayleigh number for various particle fractions under Ste* = 0.1, Sb* = 0.6

Source: Ho *et al.*

clearly shows that the contributions of latent heat absorption/release in the heated/cooled sections can be augmented with an increase of the particle faction for the range of Ra* considered except the case of $Ra^* = 10^{13}$ for which the latent heat contribution is negligibly small. Specifically, for $Ra^* = 10^{11}$ the contributions of the latent heat transport to the overall heat transfer over the heated/cooled sections are enlarged to 50.3 and 51.8 percent, respectively, as the particle fraction is increased to 15 percent. Further examination of Table III reveals that varying the modified Stefan number and/or the modified subcooling factor induces a somewhat non-monotonic variation of the latent heat contributions. There exists a threshold value of Ste* or Sb*, depending on the modified Rayleigh number and the particle fraction, over which the increasing contribution of the latent heat with the increasing Ste* or Sb* is reversed.

Conclusions

A 2D analysis of steady-state fluid flow and heat transfer in a rectangular natural circulation loop has been developed to explore efficacy of using PCM suspensions as a heat transfer enhancement medium. Key conclusions from the results presented and discussed above are as follows:

- The melting/freezing processes of the PCM particles over the heated/cooled sections are interrelated closely in the mutual bearing on the thermal conditions of their inlet suspension.

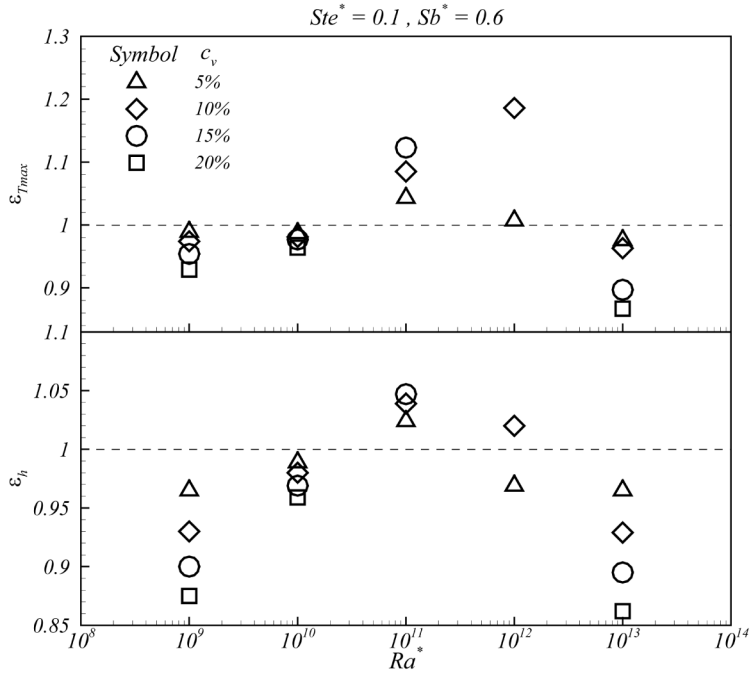

Source: Ho *et al.*

Figure 10.
Results of (a) effectiveness of reducing the maximum wall temperature $\varepsilon_{T_{max}}$ and (b) effectiveness of enhancing the average heat transfer coefficient ε_h at various modified Rayleigh numbers and particle fractions with Ste* = 0.1, Sb* = 0.6

Table II.
Effectiveness of the maximum wall temperature control the heated section and the averaged heat transfer coefficient over the cooled section for various Ste* and Sb* with c_v=10 percent

			($\varepsilon_{T_{max}}$, ε_h)		
Ra*	Ste*	Sb* = 0	Sb* = 0.6	Sb* = 1.0	Sb* = 2.0
10^{10}	0.05		(1.048, 1.030)		
	0.1	(0.936, 0.937)	(0.981, 0.980)	(1.026, 0.957)	(1.124, 0.927)
	0.5		(0.937, 0.938)		
10^{12}	0.05		(1.265, 0.995)		
	0.1	(0.990, 1.015)	(1.186, 1.020)	(2.310, 0.929)	(0.926, 0.928)
	0.5		(0.952, 0.967)		

- Among the modified Rayleigh number, the particle fraction, the modified Stefan number, and the modified subcooling factor considered here, parametric simulations indicate that each can have a significant bearing on the heat transfer characteristics and thus the thermal efficacy of the PCM suspension in the circulation loop.
- Within the parameter ranges examined, there could exists a flow regime where the latent heat absorption/release of the PCM suspension can serve effectively as the heat transfer enhancement mechanism, which is to be defined through more extensive parametric simulations. In addition, future work to address effects of the geometric parameters such as the aspect ratio; the lengths and locations of, as

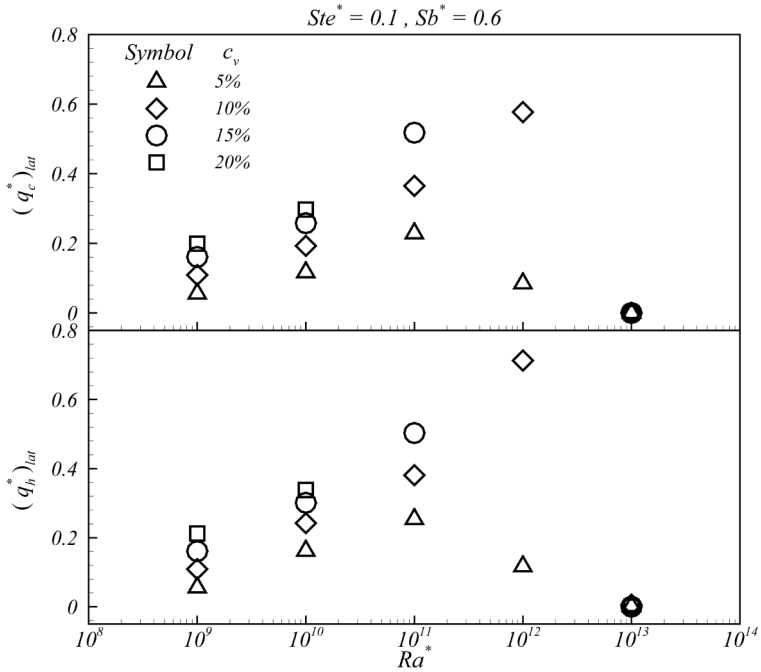

Figure 11.
Relation of latent heat contribution to the overall heat transfer with the modified Rayleigh number for various particle fractions under Ste* = 0.1 and Sb* = 0.6

Source: Ho *et al.*

Table III.
Contribution of latent heat transfer over the heated and cooled sections for various Ste* and Sb* with c_v=10 percent

		$\left[(q^*_h)_{lat}, (q^*_c)_{lat}\right]$			
Ra*	Ste*	Sb* = 0	Sb* = 0.6	Sb* = 1.0	Sb* = 2.0
10^{10}	0.05		[0.375, 0.319]		
	0.1	[0.000, 0.012]	[0.242, 0.193]	[0.300, 0.269]	[0.264, 0.294]
	0.5		[0.069, 0.050]		
10^{12}	0.05		[0.643, 0.482]		
	0.1	[0.000, 0.128]	[0.713, 0.577]	[0.064, 0.000]	[0.001, 0.000]
	0.5		[0.320, 0.339]		

well as the relative height between the heated and cooled sections is definitely needed, which are necessary steps towards developing more reliable predictive tools for system design of a circulation loop containing PCM suspension.

References

Charunyakorn, P., Sengupta, S. and Roy, S.K. (1991), "Forced convective heat transfer in microencapsulated phase change material slurries: flow in circular ducts", *Int. J. Heat Mass Transfer*, Vol. 34, pp. 819-33.

Choi, M. and Cho, K. (2000), "Liquid cooling for a multichip module using Fluorinert liquid and paraffin slurry", *Int. J. Heat Mass Transfer*, Vol. 43, pp. 209-18.

Choi, E., Cho, Y.I. and Lorsch, H.G. (1994), "Forced convective heat transfer with phase-change-material slurries: turbulent flow in a circular tube", *Int. J. Heat Mass Transfer*, Vol. 37, pp. 207-15.

Datta, P., Sengupta, P. and Roy, S.K. (1992), "Natural convection heat transfer in an enclosure with suspensions of microencapsulated phase change materials", *ASME HTD-204*, pp. 133-44.

Goel, M., Roy, S.K. and Sengupta, S. (1994), "Laminar forced convective heat transfer in microencapsulated phase change material suspensions", *Int. J. Heat Mass Transfer*, Vol. 37, pp. 593-604.

Greif, R. (1988), "Natural circulation loops", *ASME J. Heat Transfer*, Vol. 110, pp. 1243-58.

Harhira, M., Roy, S.K. and Sengupta, S. (1996), "Natural convection heat transfer from a vertical plate with phase change material suspensions", *Enhanced Heat Transfer*, Vol. 4, pp. 17-34.

Hart, R. and Thornton, F. (1982), "Microencapsulation of phase change materials", Final Report Contract No. 82-80, Ohio Department of Energy, OH.

Ho, C.J., Lin, J.F. and Chiu, S.Y. (2004), "Heat transfer of solid-liquid phase-change material suspensions in circular pipes: effects of wall conduction", *Numerical Heat Transfer Part A*, Vol. 45, pp. 171-90.

Huang, B.J. and Zelaya, R. (1988), "Heat transfer behavior of a rectangular thermosyphon loop", *ASME J. Heat Transfer*, Vol. 110, pp. 487-93.

Japikse, D. (1973), "Advances in thermosyphon technology", *Advances in Heat Transfer*, Vol. 9, pp. 1-111.

Katz, L. (1976), "Natural convection heat transfer with fluids using suspended particles which undergo phase change", PhD dissertation, Massachusetts Institute of Technology, Cambridge, MA.

Leonard, B.P. (1979), "A stable and accurate convective modeling procedure based on quadratic upstream interpolation", *Comput. Meth. Appl. Mech. Eng.*, Vol. 19, pp. 59-98.

Metrol, A., Greif, R. and Zvirin, Y. (1982), "Two-dimensional study of heat transfer and fluid flow in a natural circulation loop", *ASME J. Heat Transfer*, Vol. 104, pp. 508-14.

Sohn, C.W. and Chen, M.M. (1985), "Improvement of the performance of solar energy or waste heat utilization systems by using phase-change slurry as an enhanced heat transfer storage fluid", *ASME J. Solar Energy Eng.*, Vol. 107, pp. 229-36.

Zhang, Y. and Faghri, A. (1995), "Analysis of forced convective heat transfer in microencapsulated phase change materials", *J. Thermophys. Heat Transfer*, Vol. 9, pp. 727-32.

Zvirin, Y. (1981), "A review of natural circulation loops in pressurized water reactors and other systems", *Nuclear Engineering Design*, Vol. 67, pp. 203-25.